

## Supporting information

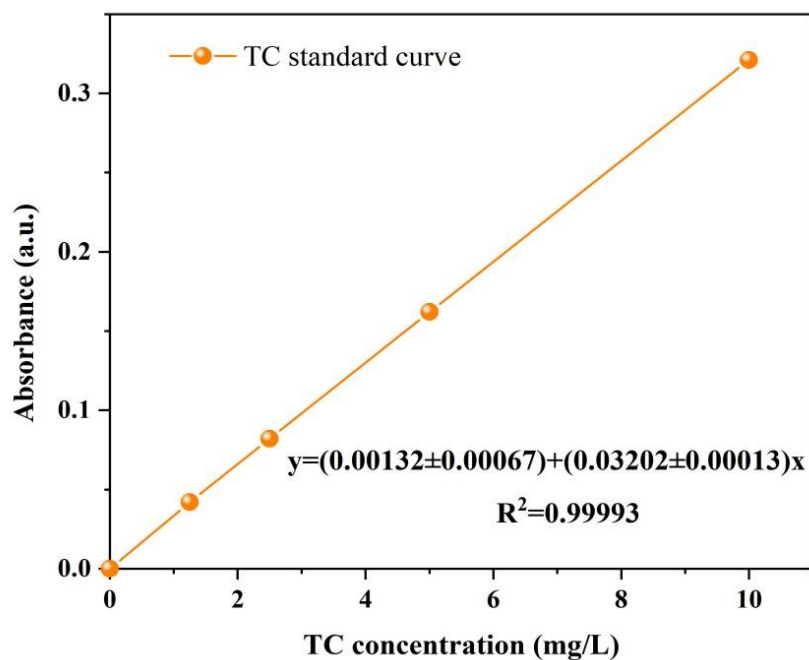


Figure S1. TC standard curve for absorbance and concentration.

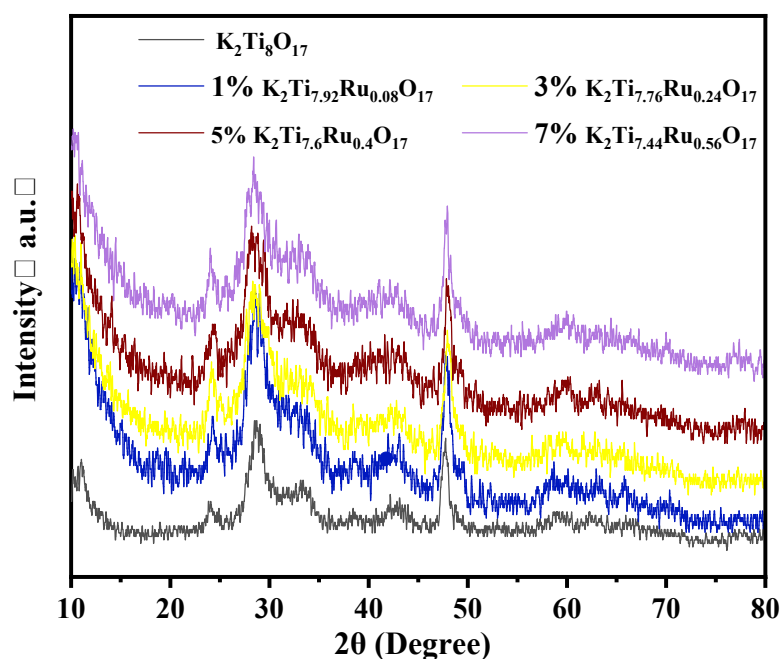


Figure S2. The powder XRD patterns of the  $K_2Ti_{8-x}Ru_xO_{17}$  precursors with different doping concentrations (Ru:(Ru+Ti)=0%, 1%, 3%, 5%, 7%).

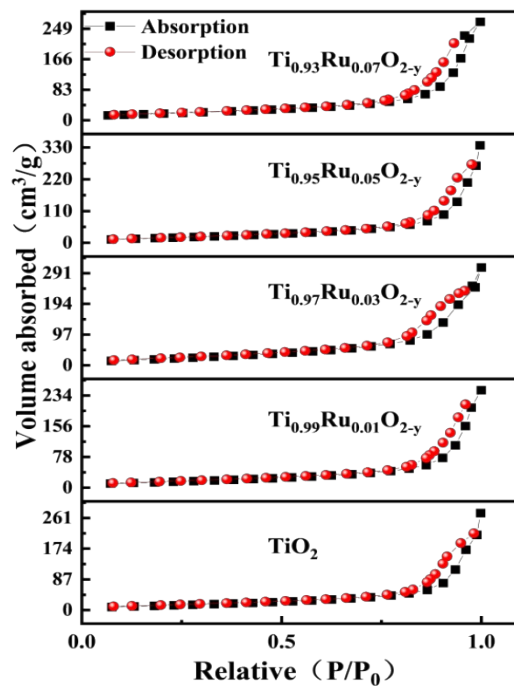


Figure S3.  $N_2$  adsorption-desorption isotherms of  $Ti_{1-x}Ru_xO_{2-y}$  with different molar ratios (Ru:(Ru+Ti)=0%, 1%, 3%, 5%, 7%).

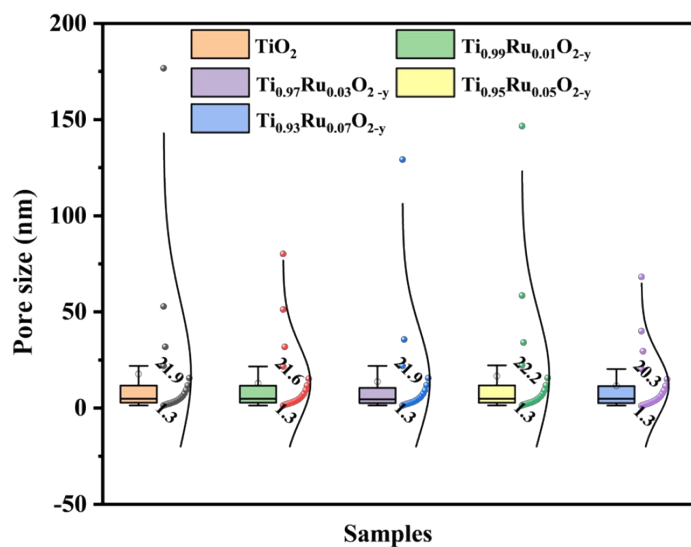


Figure S4. Pore size distribution of  $Ti_{1-x}Ru_xO_{2-y}$  with different molar ratios (Ru:(Ru+Ti)=0%, 1%, 3%, 5%, 7%).

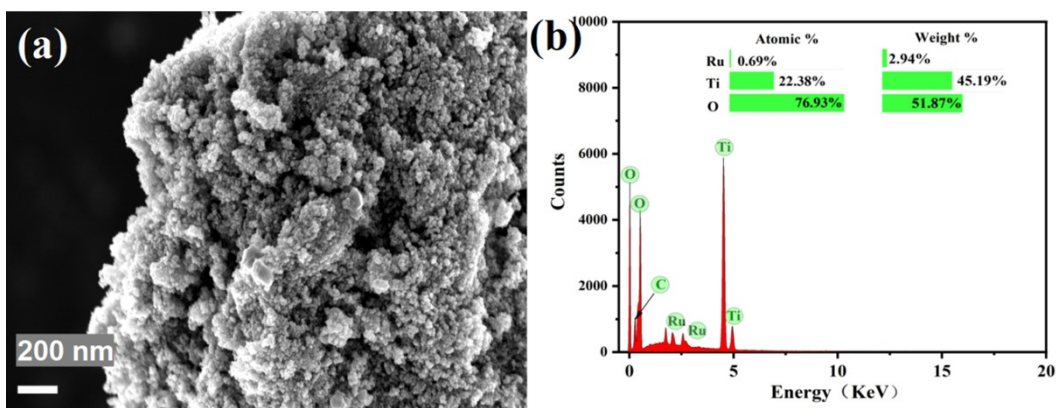


Figure S5. (a) SEM of  $\text{Ti}_{0.95}\text{Ru}_{0.05}\text{O}_{2-y}$ . (b) EDS of  $\text{Ti}_{0.95}\text{Ru}_{0.05}\text{O}_{2-y}$ .

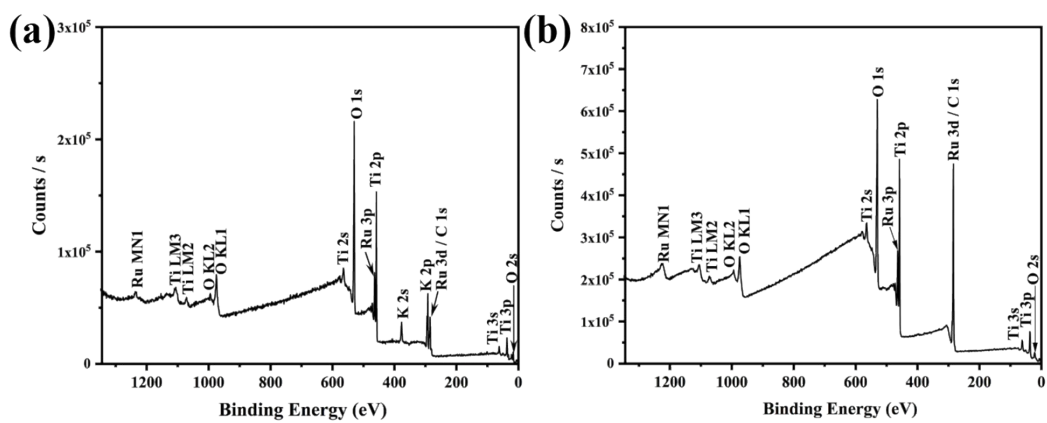


Figure S6. XPS survey spectra of (a)  $\text{K}_2\text{Ti}_{7.6}\text{Ru}_{0.4}\text{O}_{17}$  and (b)  $\text{Ti}_{0.95}\text{Ru}_{0.05}\text{O}_{2-y}$ .

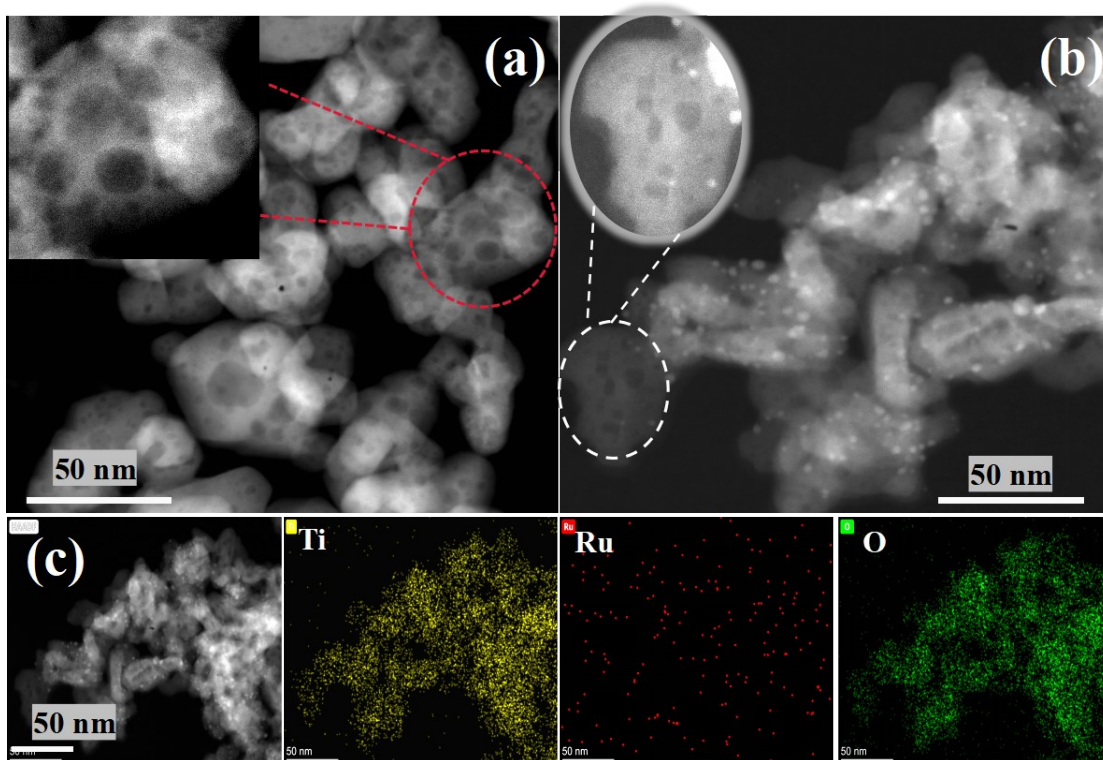


Figure S7. (a) High-angle annular dark-field scanning transmission electron microscopy (HAADF-STEM) of  $\text{TiO}_2$ . (b) HAADF-STEM of  $\text{Ti}_{0.95}\text{Ru}_{0.05}\text{O}_{2-y}$ . (c) Mapping of  $\text{Ti}_{0.95}\text{Ru}_{0.05}\text{O}_{2-y}$ .

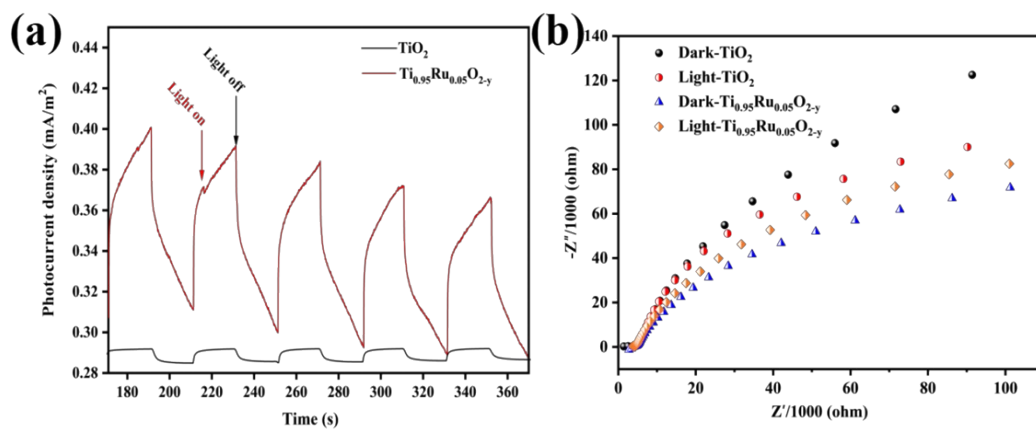


Figure S8. (a) Transient photocurrent response and (b) the EIS Nyquist plots of  $\text{TiO}_2$  and  $\text{Ti}_{0.95}\text{Ru}_{0.05}\text{O}_{2-y}$ .

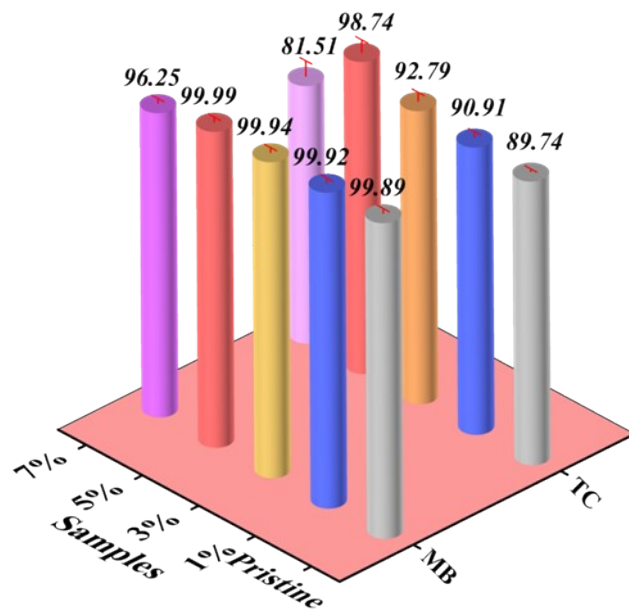


Figure S9 The photocatalytic degradation rate statistics of TC and MB by  $Ti_{1-x}Ru_xO_{2-y}$ .

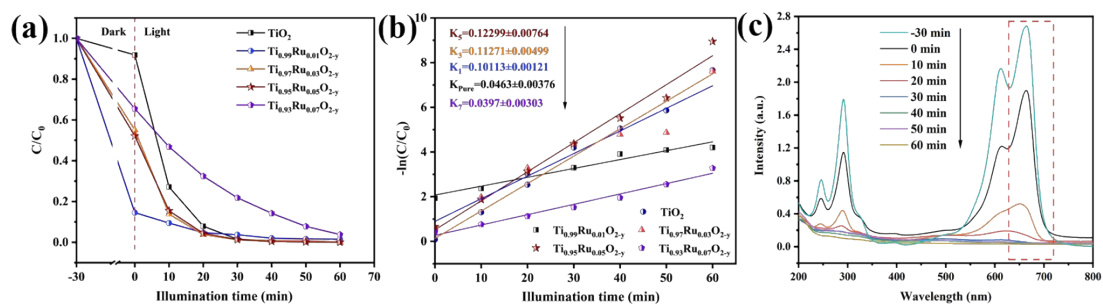


Figure S10. Photocatalytic degradation of MB of  $Ti_{1-x}Ru_xO_{2-y}$  under simulated sunlight: (a) degradation efficiency of MB (Initial conditions: 20 mg/L MB, 1 g/L catalysts.). (b) reaction kinetics of MB photodegradation curve. (c) UV-vis absorption spectrum of  $Ti_{0.95}Ru_{0.05}O_{2-y}$  photocatalytic degradation of MB.

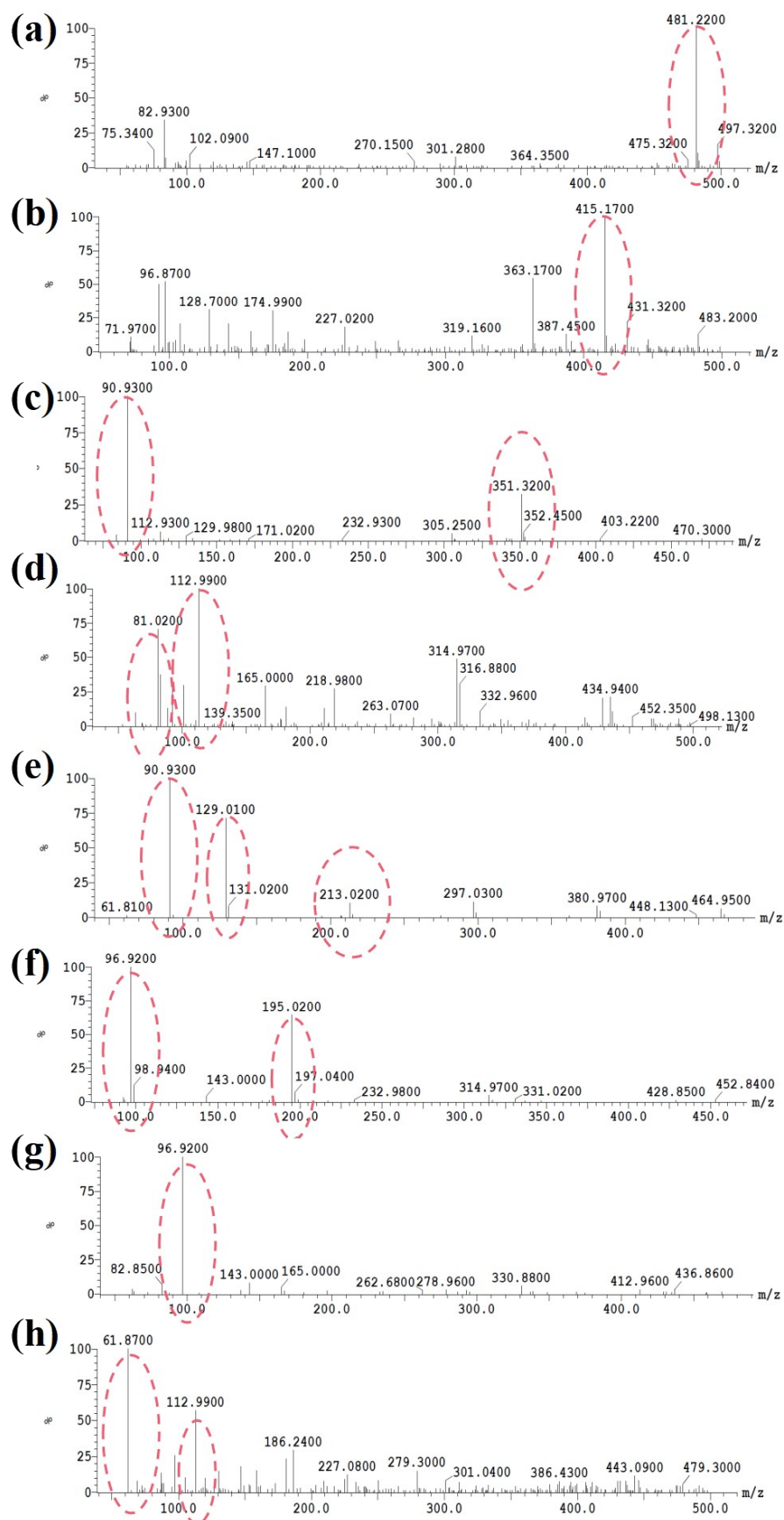


Figure S11 HPLC-MS of photocatalytic degradation TC by  $\text{Ti}_{0.95}\text{Ru}_{0.05}\text{O}_{2-y}$  in different reaction time periods. (a) 30 min, peak time: 7.38 min. (b) 40 min, peak time: 10.50 min. (c) 40 min, peak

time: 15.07 min. (d) 70 min, peak time: 2.52 min. (e) 50 min, peak time: 8.72 min. (f) 50 min, peak time: 1.67 min. (g) 70 min, peak time: 1.68 min. (h) 50 min, peak time: 7.82 min.

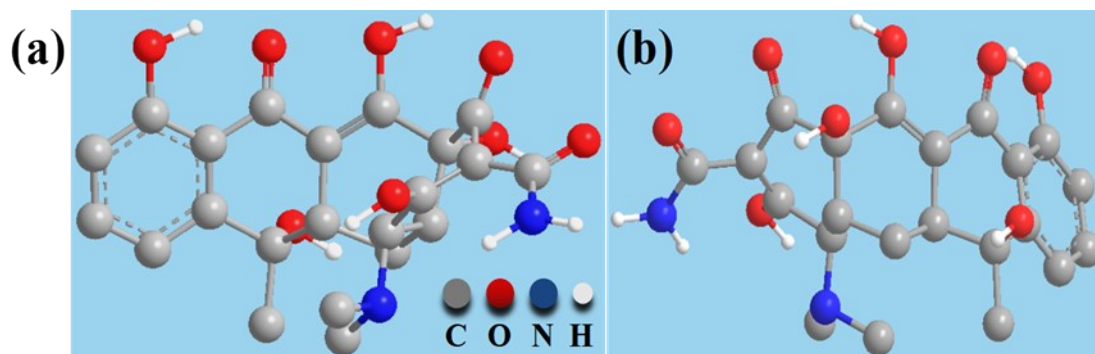


Table S1. Specific surface area of  $Ti_{1-x}Ru_xO_{2-y}$  with different molar ratios.

$Ti_{1-x}Ru_xO_{2-y}$	$TiO_2$	$Ti_{0.99}Ru_{0.01}O_{2-y}$	$Ti_{0.97}Ru_{0.03}O_{2-y}$	$Ti_{0.95}Ru_{0.05}O_{2-y}$	$Ti_{0.93}Ru_{0.07}O_{2-y}$
Specific surface area ( $m^2/g$ )	55.74	73.74	69.34	71.86	79.63

Table S2. Related parameters of ICP-AES

Samples	Element	Weight/g	Volume/ ml	Dilution factor	Instrument indication mg/L	Concentration/ mg/kg
$K_2Ti_{7.6}Ru_{0.4}O_{17}$	Ru	0.0408	50	50	0.592	36116.1208
$K_2Ti_{7.6}Ru_{0.4}O_{17}$	Ti	0.0408	50	50	5.7969	355203.6788
$Ti_{0.95}Ru_{0.05}O_{2-y}$	Ru	0.0563	50	10	7.225	64165.8035
$Ti_{0.95}Ru_{0.05}O_{2-y}$	Ti	0.0563	50	50	14.1216	627069.8474

Table S3. The degradation rates of TC, kinetic constants k value and correlation coefficient under different catalysts.

Photocatalysts	Light source	Degradation rate	k /min <sup>-1</sup>	References
$Bi_2WO_6$	Visible	77.1%	0.021	[24]
$NaTaO_3@WO_3$	Visible	60.9%	None	[25]
$Sb_2O_3$	UV	80.6%	None	[26]
g- $C_3N_4/LaCoO_3$	UV-Vis	92.0%	0.019	[27]
$Pb_4(BO_3)_2SO_4$	UV-Vis	90.6%	0.216	[28]
l- $ZnFe_2O_4$	Visible	84.1%	0.067	[29]
N- $TiO_2$	UV	94.8%	0.038	[30]
$Ag@SnO_2/TiO_2$	Simulated sunlight	83.1%	0.057	[31]
$Ag-Bi_2MoO_6/TiO_2$	Simulated sunlight	90.8%	0.020	[32]
$TiO_2/GO$	Visible	53.6%	None	[33]
$Ti_{0.95}Ru_{0.05}O_{2-y}$	Simulated sunlight	98.7%	0.078	This work